First-principles calculations of atomic and electronic structure of $SrTiO_3$ (001) and (011) surfaces

R. I. Eglitis and David Vanderbilt
Department of Physics and Astronomy, Rutgers University, 136 Frelinghuysen Road, Piscataway, New Jersey 08854-8019, USA
(Received 28 February 2008; revised manuscript received 10 April 2008; published 6 May 2008)

We present and discuss the results of the calculations of surface relaxation and rumpling on $SrTiO_3$ (001) and (011) surfaces. We consider both SrO and TiO_2 terminations of the (001) surface, and three terminations (Sr, TiO, and O) of the polar (011) surface. The calculations are based on hybrid Hartree–Fock and density-functional theory exchange functionals by using Becke's three-parameter method combined with the nonlocal correlation functionals of Perdew and Wang. We find that all top-layer atoms for TiO_2 and SrO-terminated $SrTiO_3$ (001) surfaces relax inward, with the exception of SrO-terminated surface O atoms, whereas all second-layer atoms relax outward. The surface rumpling for the TiO-terminated $SrTiO_3$ (011) surface, which is 11.28% of the bulk lattice constant, is considerably larger than the relevant surface rumplings for SrO and TiO_2-terminated (001) surfaces. The surface rumplings for the SrO and TiO_2-terminated (001) surfaces are in excellent agreement with relevant low-energy electron diffraction and reflection high-energy electron diffraction experimental data, and the surface relaxation energies on both surfaces are similar. In contrast, the different terminations of the (011) surface lead to large differences in relaxation energies. The O-terminated (011) surface has the lowest surface relaxation energy (−1.32 eV). The TiO-terminated (011) surface has a much higher surface relaxation energy of −1.55 eV, while the Sr-terminated (011) surface has the highest surface relaxation energy (−1.95 eV). Our calculations indicate a considerable increase in the Ti-O bond covalency (0.130*e*) near the TiO-terminated (011) surface relative to the bulk (0.088*e*), which is much larger than that for the (001) surface (0.118*e*). The Ti-O bond populations are considerably larger in the direction perpendicular to the TiO-terminated (011) surface (0.188*e*) than in the plane (0.130*e*).

DOI: 10.1103/PhysRevB.77.195408 PACS number(s): 68.35.Ct, 68.35.Md, 68.47.Gh

I. INTRODUCTION

Oxide perovskites are promising for many device applications because of their diverse physical properties,[1] both in bulk and thin-film form.[1,2] In particular, titanate perovskites are of great interest for their ferroelectric and piezoelectric properties, their electrochemical behavior, and their use in electrodes and sensors. $SrTiO_3$ is among the best studied and most important of the perovskite titanates, as it is widely used as a dielectric and as a substrate for growth of thin films or superlattices of other functional perovskite or related (e.g., high-T_c) materials. For these reasons, a detailed understanding of the surface structure and electronic properties is of primary importance.

It is not surprising that this high technological importance has motivated several *ab initio*[3–18] and classical shell-model[19,20] studies of the (001) surface of $SrTiO_3$. The (001) surface relaxation and rumpling have also been experimentally studied by means of low-energy electron diffraction (LEED), reflection high-energy electron diffraction (RHEED), medium energy ion scattering (MEIS), and surface x-ray diffraction (SXRD) measurements.[21–26] The most recent experimental studies on the $SrTiO_3$ surfaces include a combination of XPS, LEED, and time-of-flight scattering and recoil spectrometry[27] (TOF-SARS) as well as metastable impact electron spectroscopy.[28] In these recent studies, well-resolved 1×1 LEED patterns were obtained for the TiO_2-terminated $SrTiO_3$ (001) surface. Simulations of the TOF-SARS azimuthal scans indicate that the O atoms are situated 0.1 Å above the Ti layer (surface plane) in the case of the TiO_2-terminated $SrTiO_3$ (001) surface. There is general agreement between theory and LEED and RHEED experiments on the larger rumpling for the SrO termination. However, there is a disagreement about the direction of surface O atom displacements on the TiO_2-terminated $SrTiO_3$ (001) surface, which is probably due to neglect in the theory of the anharmonic vibrations of the surface atoms, especially Ti. On the other hand, several diffraction experiments clearly contradict each other, most likely because of differences in sample preparation or different interpretations of indirect experimental data on the atomic surface relaxations.[17] Resonance photoemission[29] from Ti 3*d* states above the Ti 3*p* absorption threshold has been used to extract regions of Ti 3*d*-state hybridization in the O 2*p* valence band of bulk $SrTiO_3$ and of the surface of $SrTiO_3$ (001). An enhanced covalent mixing on the surface is found.[29]

ABO_3 perovskite (011) surfaces, in general, and $SrTiO_3$ (011) surfaces, in particular, are considerably less well studied than the corresponding (001) surfaces. The first *ab initio* calculations of the $SrTiO_3$ (011) surface was performed by Bottin *et al.*,[30] who carried out a systematic first-principles study of the electronic and atomic structure of several (1×1) terminations of the (011) surface. The electronic structures of the stoichiometric SrTiO and O_2 terminations were characterized by marked differences with respect to the bulk, as a consequence of the polarity compensation. One year later, Heifets *et al.*[31] performed *ab initio* Hartree–Fock calculations for four possible terminations (TiO, Sr, and two kinds of O terminations) of the $SrTiO_3$ (011) surface. Heifets *et al.*[32] also investigated the atomic structure and charge redistribution for different terminations of the $BaZrO_3$ (011) surfaces by using density-functional theory, finding that while the O-terminated (011) surface had the smallest cleavage energy among (011) surfaces, this value was still twice as large as for the formation of a pair of complimentary

 ©2008 The American Physical Society

(001) surfaces. Finally, Eglitis and Vanderbilt[33] performed *ab initio* calculations for the technologically important $BaTiO_3$ and $PbTiO_3$ (011) surfaces.

In this paper, we analyze in detail the structural and electronic properties of the $SrTiO_3$ (001) and (011) surfaces. For the better-studied (001) surfaces, we address, in particular, the contradictory experimental results for this surface, and we independently check the reports of enhanced Ti-O covalent bonding near the surface.[29] Then, since only two *ab initio* studies have been reported up to now dealing with the $SrTiO_3$ (011) surfaces,[30,31] we perform detailed predictive calculations for several terminations of this surface, with an emphasis on the effect of the surface relaxation and rumpling, surface energies, and the charge redistributions and changes in bond strength that occur at the surface. We chose the hybrid B3PW functional for our current study because it yields excellent results for the bulk lattice constant and bulk modulus of $SrTiO_3$, $BaTiO_3$, $PbTiO_3$, CaF_2, and BaF_2.[9,34–36] For example, for bulk $SrTiO_3$, our calculated lattice constant of 3.904 Å is in excellent agreement with the experimental value of 3.89 Å, whereas local density approximation (LDA) is usually[37] about 1% too small[38–41] and Hartree–Fock (3.93 Å) is about 1% too large.[31]

II. COMPUTATIONAL METHOD

To perform the first-principles DFT-B3PW calculations, we used the CRYSTAL-2003 computer code.[42] This code employs Gaussian-type functions (GTFs) localized on atoms as the basis for an expansion of the crystalline orbitals. The features of the CRYSTAL-2003 code that are most important for this study are its ability to calculate the electronic structure of materials within both Hartree–Fock (HF) and Kohn–Sham Hamiltonians, and its implementation of an isolated two-dimensional (2D) slab model without artificial repetition along the z axis. However, in order to employ the linear combination of atomic orbitals (LCAO)-GTF method, it is desirable to have optimized basis sets. Such an optimized basis set for $SrTiO_3$ was developed and discussed in Ref. 34. In the present work, we have adopted this new basis set, which differs from that used in previous calculations[8,9] by inclusion of polarizable d orbitals on the O ions. It was shown[34] that this leads to better agreement of the calculated lattice constant and bulk modulus with experimental data.

Our calculations were performed by using the hybrid exchange-correlation B3PW functional involving a mixture of nonlocal Fock exact exchange, LDA exchange, and Becke's gradient corrected exchange,[43] combined with the nonlocal gradient-corrected correlation potential by Perdew and Wang.[44] The Hay–Wadt small-core effective core pseudopotentials (ECPs) were adopted for Ti and Sr atoms.[45] The small-core ECPs replace only the inner core orbitals, while orbitals for subvalence electrons as well as for valence electrons are calculated self-consistently. Oxygen atoms were treated with an all-electron basis set.

The reciprocal space integration was performed by sampling the Brillouin zone with an 8×8 Pack–Monkhorst mesh.[46] To achieve high accuracy, large enough tolerances of 7, 8, 7, 7, and 14 were chosen for the Coulomb overlap, Coulomb penetration, exchange overlap, first exchange pseudo-overlap, and second exchange pseudo-overlap, respectively.[42]

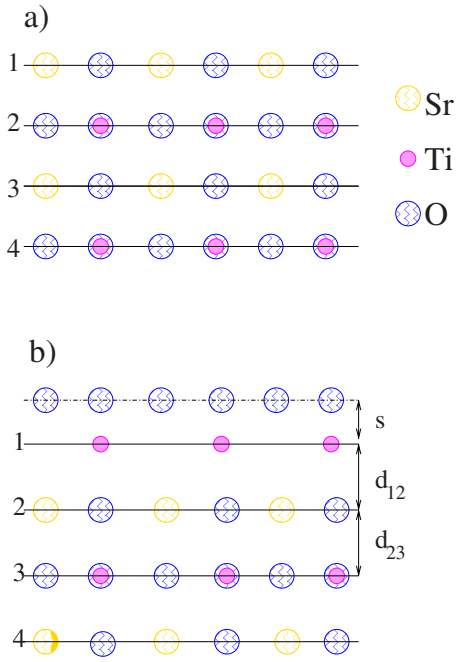

FIG. 1. (Color online) Side view of $SrTiO_3$ (001) surfaces. (a) SrO-terminated surface. (b) TiO_2-terminated surface, with definitions of surface rumpling s and the near-surface interplanar separations d_{12} and d_{23}.

The $SrTiO_3$ (001) surfaces were modeled with 2D slabs consisting of several planes perpendicular to the [001] crystal direction, as illustrated in Fig. 1. The CRYSTAL-2003 code allowed us to avoid artificial periodicity along the z direction and to perform simulations for stand-alone 2D slabs. To simulate $SrTiO_3$ (001) surfaces, we used slabs consisting of seven alternating TiO_2 and SrO layers, with a mirror symmetry through the middle of the slab. One of these slabs was terminated by SrO planes and contained 17 atoms in the supercell, while the second was terminated by TiO_2 planes and contained 18 atoms. These slabs are nonstoichiometric, with unit cell formulas $Sr_4Ti_3O_{10}$ and $Sr_3Ti_4O_{11}$, respectively. The sequences of layers for the two $SrTiO_3$ (001) surfaces are shown in Fig. 1.

Turning next to the polar $SrTiO_3$ (011) surface, we note that the crystal is composed of charged O-O or SrTiO planes, as shown in Fig. 2. If one assumes nominal ionic charges of Sr^{2+}, Ti^{4+}, and O^{2-}, the O-O, and SrTiO layers have charges of ∓4, respectively. Thus, a simple cleavage terminating on an O-O layer would leave a net negative surface charge, while a termination on a SrTiO layer would leave a net positive charge. This would lead to a large dipole for an asymmetric slab like that of Fig. 3(a) or a net charge in the supercell in the case of Figs. 3(b) and 3(c). The surfaces might become metallic in order to avoid the infinite electrostatic energy arising from such surface charges, but in any case, the surface energy would be expected to be quite high.[30,47–50] It is much more likely that the surface would reconstruct in order to restored the neutrality of the surface layers.

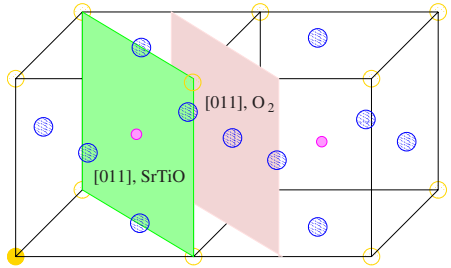

FIG. 2. (Color online) Sketch of the cubic $SrTiO_3$ perovskite structure showing two (011) cleavage planes that give rise to charged SrTiO and O_2 (011) surfaces.

We thus construct surface slab models as follows. Starting from the symmetric SrTiO-terminated slab in Fig. 3(c), we can remove the Sr atom from each surface to obtain the seven-layer (16-atom) TiO-terminated slab shown in Fig. 3(d). We can alternatively remove TiO units from each surface and obtain the seven-layer (14-atom) Sr-terminated slab, as shown in Fig. 3(e). Finally, we can also start from the symmetric O_2-terminated slab in Fig. 3(b) and remove one of each two surface O atoms to obtain the seven-layer (15-atom) O-terminated slab model in Fig. 3(f). We use the slab models in Figs. 3(d)–3(f) for our subsequent calculations. Note that the O-terminated slab in Fig. 3(f) is the only one of the three that is stoichiometric but all have symmetry through the middle of the slab and have nonpolar surface terminations. For a more in-depth discussion of stoichiometric and nonstoichiometric (011) surface terminations of this crystal (see Ref. 30).

In order to confirm that our slabs are thick enough to give meaningful results, we tested the convergence of energy with

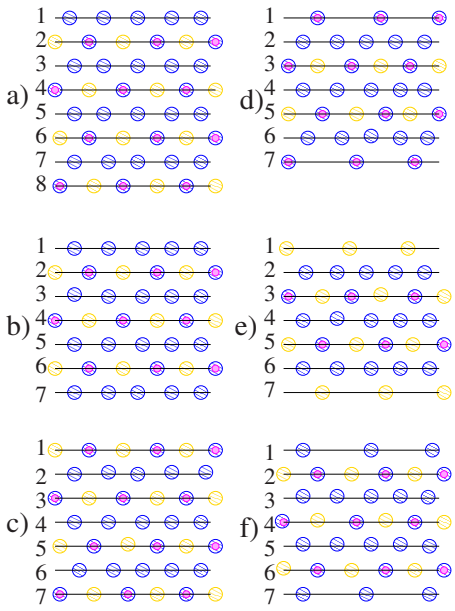

FIG. 3. (Color online) Possible (011) surface slab models considered in the text. [(a)–(c)] Slabs obtained by simple cleavage, yielding mixed, O-terminated, and SrTiO-terminated polar surfaces, respectively. [(d)–(f)] Slabs with nonpolar TiO-terminated, Sr-terminated, and O-terminated surfaces, respectively.

TABLE I. Computed effective charges Q and bond populations P of atoms in bulk $SrTiO_3$.

Ion	Property	B3PW
Sr	Q	1.871
	P	−0.010
O	Q	−1.407
	P	0.088
Ti	Q	2.351

slab thickness. To do so, we computed the energy change when one $SrTiO_3$ layer is added to the slab, which is referenced by subtracting the bulk energy per cell in order to get meaningful surface energies.[51,52] The convergence is considered to be achieved when this energy difference is smaller than 1 mHa. In our case, the slabs containing seven layers satisfy this criterion; the energy change as defined above was found to be less that 0.01 eV between seven-layer and nine-layer slabs.

III. RESULTS OF CALCULATIONS

A. $SrTiO_3$ bulk atomic and electronic structure

As a starting point for our calculations, we calculated the $SrTiO_3$ bulk lattice constant to be 3.904 Å, which is in almost perfect agreement with the experimental result extrapolated to 0 K (3.89 Å).[53] We used the theoretical $SrTiO_3$ bulk lattice constant in the following surface structure calculations. To characterize the chemical bonding and covalency effects, we used a standard Mulliken population analysis for the effective atomic charges Q and other local electronic-structure properties (bond orders, atomic covalencies, and full valencies), as described, for example, in Refs. 54 and 55. Our calculated static effective charges for bulk $SrTiO_3$ are $1.871e$ for the Sr atom, $2.351e$ for the Ti atom, and $-1.407e$ for the O atom, while the population of the chemical bond between Ti and O atoms is $0.088e$ (see Table I).

B. $SrTiO_3$ (001) surface atomic and electronic structure

In the present $SrTiO_3$ (001) calculations that use the hybrid B3PW method, we allowed atoms in the two outermost surface layers to relax along the z axis (by symmetry the atoms have no forces along the x or y axis). The resulting atomic displacements for the TiO_2- and SrO-terminated (001) surfaces are shown in Table II. For the TiO_2-terminated surface, we find that both the Ti and the O atoms in the first surface layer relax inward (i.e., toward the bulk), whereas in the case of the SrO-terminated surface, the upper-layer Sr atoms relax inward, while the upper-layer O atoms relax outward. For both terminations, outward relaxation of all of the atoms in the second layer is found. A comparison to the surface atomic displacements obtained by other theoretical methods is also given in Table II. This shows that the direction of the atomic displacements calculated by quite different *ab initio* and the classical shell-model methods is always the same for both first-layer atoms, as well as for the second-

TABLE II. Calculated atomic relaxation (in percent of bulk lattice constant) for SrO and TiO_2 terminated $SrTiO_3$ (001) surfaces. Positive (negative) values refer to displacements outward from (inward to) the surface.

	SrO terminated					TiO_2 terminated				
N	Ion	This work	SM[a]	LDA[b]	LDA[c]	Ion	This work	SM[a]	LDA[b]	LDA[c]
1	Sr	−4.84	−7.10	−5.7	−6.66	Ti	−2.25	−2.96	−3.4	−1.79
	O	0.84	1.15	0.1	1.02	O	−0.13	−1.73	−1.6	−0.26
2	Ti	1.75	1.57	1.2	1.79	Sr	3.55	3.46	2.5	4.61
	O	0.77	0.87	0.0	0.26	O	0.57	−0.21	−0.5	0.77
3	Sr		−1.42	−1.2	−1.54	Ti		−0.60	−0.7	−0.26
	O		0.70	−0.1	0.26	O		−0.29	−0.5	0.26

[a]Reference 19.
[b]Reference 17.
[c]Reference 16.

layer Ti atoms, but the displacement magnitudes are quite different.

In order to compare the calculated $SrTiO_3$ (001) surface structures to the available experimental results, the amplitudes of the surface rumpling s (the relative displacement of oxygen with respect to the metal atom in the surface layer) and the changes in the interlayer distances Δd_{ij} (where i and j are the layer numbers) are presented in Table III. Our calculations of the interlayer distances are based on the positions of relaxed metal ions, which are known to be much stronger electron scatterers than oxygen ions.[21] The agreement is quite good for all theoretical methods, which give the same sign for both the surface rumpling and changes of the interlayer distances. The amplitude of the surface rumpling for the SrO-terminated $SrTiO_3$ (001) surface is predicted to be much larger than that for TiO_2-terminated surface. As one can see from Table III, both SrO and TiO_2 terminated $SrTiO_3$ (001) surfaces display a reduction of the interlayer distance Δd_{12} and an expansion of Δd_{23}.

The calculated surface rumpling amplitudes s for both (001) surface terminations are in qualitative agreement with the available LEED, RHEED, MEIS, and SXRD experimental results.[21,22,25,26] Unfortunately, the calculated changes in interlayer distances Δd_{ij} are in disagreement with the LEED experimental data[21] for the TiO_2 terminated (001) surface, which show an expansion of the interlayer distance Δd_{12} and a reduction of the interlayer distance Δd_{23}, while on the contrary, all *ab initio* and classical shell-model calculations predict a reduction of the interlayer distance Δd_{12} and an expansion of Δd_{23}. Moreover, as can be seen from Table III, the experiments contradict each other regarding the sign of Δd_{12} and Δd_{23} for the SrO-terminated surface, as well as for Δd_{23} of the TiO_2-terminated surface.

Another discrepancy between theory and experiment is that the LEED, RHEED, and MEIS experiments[21,22,25] demonstrate that the topmost layer oxygen atoms always move outward from the surface, whereas all *ab initio* and classical shell-model calculations for the TiO_2-terminated $SrTiO_3$ (001) surface predict that the oxygen atoms relax toward the bulk. It is important to also note the contradiction between the LEED, RHEED, and MEIS experiments[21,22,25] and a recent SXRD[26] experiment, wherein oxygen atoms are predicted to move inward for both surface terminations, reaching a very large rumpling amplitude up to 12.8% of the bulk

TABLE III. Surface rumpling s and relative displacements Δd_{ij} (in percent of bulk lattice constant) for the three near-surface planes of SrO and TiO_2 terminated $SrTiO_3$ (001) surfaces.

	SrO terminated			TiO_2 terminated		
	s	Δd_{12}	Δd_{23}	s	Δd_{12}	Δd_{23}
This study	5.66	−6.58	1.75	2.12	−5.79	3.55
Ab initio[a]	5.8	−6.9	2.4	1.8	−5.9	3.2
Ab initio[b]	7.7	−8.6	3.3	1.5	−6.4	4.9
Shell model[c]	8.2	−8.6	3.0	1.2	−6.4	4.0
LEED experiment[d]	4.1 ± 2	-5 ± 1	2 ± 1	2.1 ± 2	1 ± 1	-1 ± 1
RHEED experiment[e]	4.1	2.6	1.3	2.6	1.8	1.3
MEIS experiment[f]				1.5 ± 0.2	0.5 ± 0.2	
SXRD experiment[g]	1.3 ± 12.1	-0.3 ± 3.6	-6.7 ± 2.8	12.8 ± 8.5	0.3 ± 1	

[a]Reference 17.
[b]Reference 16.
[c]Reference 19.
[d]Reference 21.
[e]Reference 22.
[f]Reference 25.
[g]Reference 26.

TABLE IV. Calculated absolute magnitudes of atomic displacements D (in Å), the effective atomic charges Q (in e), and the bond populations P between nearest Me-O atoms (in e) for the TiO_2 and SrO terminated $SrTiO_3$ (001) surfaces.

Layer	Property	Ion	TiO_2 terminated	Ion	SrO terminated
1	D	Ti	−0.088	Sr	−0.189
	Q		2.291		1.846
	P		0.118		−0.006
	D	O	−0.005	O	0.033
	Q		−1.296		−1.522
	P		−0.014		0.074
2	D	Sr	0.139	Ti	0.068
	Q		1.850		2.363
	P		−0.008		0.078
	D	O	0.022	O	0.030
	Q		−1.365		−1.450
	P		0.080		−0.010
3	Q	Ti	2.348	Sr	1.875
	P		0.096		−0.012
	Q	O	−1.384	O	−1.429
	P		−0.010		0.084

lattice constant for the TiO_2-terminated surface. The reasons for such discrepancies between the different experimental data are not clear, but the matter is comprehensively discussed in Refs. 17 and 26. In any case, we conclude that the disagreement in some cases between theoretical *ab initio* and shell-model results on one side and experimental results on the other side should not be too seriously taken until the internal inconsistencies in the experimental results are resolved.

The atomic displacements D, effective static atomic charges Q, and bond populations P between nearest metal and oxygen atoms for the $SrTiO_3$ (001) surfaces are given in Table IV. The major effect observed here is a strengthening of the Ti-O chemical bond near the TiO_2-terminated (001) surface. Note that the Ti and O effective charges in bulk $SrTiO_3$ of $2.351e$ and $-1.407e$, respectively (see Table I), are much smaller than those expected in an ionic model. The Ti-O bond population for the TiO_2-terminated (001) surface is $0.118e$ (see Table IV), which is considerably larger than the value of $0.088e$ in the bulk. In contrast, the Sr-O bond populations are very small. The lack of covalency in the Sr-O bond is also seen in the Sr effective charges of $1.871e$ in the bulk and $1.846e$ on the SrO-terminated (001) surface, which are close to the formal ionic charge of $2e$.

C. $SrTiO_3$ (011) surface atomic structure

Our calculated atomic relaxations for the $SrTiO_3$ (011) surfaces are shown in Table V. An idea of the nature of the relaxed (011) surfaces can be obtained from Figs. 3(d)–3(f). The first-layer metal atoms for the TiO- and Sr-terminated (011) surfaces strongly relax inward by $0.0769a$ for Ti and even more strongly by $0.1281a$ for Sr, whereas the O atoms on the TiO-terminated (011) surface relax outward by $0.0359a$. (Here, a is the bulk lattice constant.) The O atoms in the top layer of the O-terminated (011) surface also move inward by $0.0661a$. The results calculated by using the classical shell model[19] for the TiO, O, and Sr-terminated (011) surface upper layers display the same atomic displacement directions as our calculations, but in most cases, the atomic displacement magnitudes are considerably larger. Also, for the second- and third-layer atoms on the TiO and Sr-terminated (011) surface, the directions of the atomic displacements calculated by using the hybrid B3PW method coincide in all of the cases with those calculated by using the classical shell model,[19] but the displacements calculated from the latter method are almost always larger. Only the third-layer O atom displacement for the Sr-terminated (011) surface ($0.0108a$) calculated by using the hybrid B3PW method is larger than the displacement ($0.0025a$) obtained by the means of the classical shell model.[19]

For the O-terminated (011) surface, the atomic displacement directions calculated by using the hybrid B3PW method are mostly the same as those calculated by the shell-model method,[19] but in same cases, there are also qualitative differences. For example, according to our B3PW results, the Sr atoms in the second layer of this surface move along the surface by $0.0085a$ and also slightly inward by $0.0118a$. In contrast, the same atom, according to the shell-model calculation,[19] moves along the surface in the opposite direction by $0.1079a$ and also outward by $0.0410a$. The atomic displacements in the third plane from the surface for all three terminations of the (011) surface are still large. This is in sharp contrast to our results for the neutral (001) surfaces in Table II, where the atomic displacements converged very quickly and were already negligible in the third layer.

Our calculated surface rumpling s for the TiO-terminated (011) surface and the relative displacements of the three top

TABLE V. Atomic relaxation of the $SrTiO_3$ (011) surface (in per cent of the bulk lattice constant) for the three terminations calculated by means of the *ab initio* B3PW method. A positive sign corresponds to outward atomic displacements.

Layer	Ion	Δz	Δy	Δz (SM)	Δy (SM)
		TiO-terminated $SrTiO_3$ (011) surface			
1	Ti	−7.69		−5.99	
1	O	3.59		8.48	
2	O	−0.51		−1.72	
3	Sr	−2.10		−6.96	
3	O	−2.56		−4.10	
3	Ti	0.16		2.14	
		Sr-terminated SrTiO3 (011) surface			
1	Sr	−12.81		−19.07	
2	O	1.02		3.18	
3	Ti	−0.04		−0.89	
3	O	−1.08		−0.25	
3	Sr	0.26		4.67	
		O-terminated $SrTiO_3$ (011) surface			
1	O	−6.61	−0.14	−14.20	−8.54
2	Ti	−1.02	−4.35	−2.37	−8.27
2	Sr	−1.18	0.85	4.10	−10.79
2	O	1.79	6.40	5.71	8.20
3	O	−0.79	2.10	−11.06	−11.01

layers Δd_{12} and Δd_{23} for TiO and O-terminated (011) surfaces are listed in Table VI. For the TiO-terminated surface, our computed B3PW surface rumplings (11.28%) and those computed from the shell model[19] (14.47%) are comparable and very large. This arises, according to the results of our calculations, from a combination of a strong O atom outward displacement by 3.59% and an even stronger Ti atom inward displacement by 7.69%. This (011) surface rumpling is much larger than that found for the (001) surfaces. Our B3PW-calculated reduction of relative distances Δd_{12} between the first and second layers for the TiO- and O-terminated (011) surfaces (−7.18% and −5.59%, respectively) are more that ten times larger than the reduction of relative distances Δd_{23} between the second and third layer (−0.67% and −0.23%). The corresponding interlayer distance reductions computed from the classical shell model[19] are also large and comparable to our *ab initio* results. There is also one quantitative difference between our *ab initio* B3PW calculations and the shell-model results, namely, that the latter[19] predicts an expansion of the interlayer distance Δd_{23} for the O-terminated (011) surface, while our calculations predict a reduction of the same interlayer distance.

D. $SrTiO_3$ surface energies

In the present work, we define the unrelaxed surface energy of a given surface termination Λ to be one-half of the energy needed to cleave the crystal rigidly into an unrelaxed surface Λ and an unrelaxed surface with the complementary termination Λ'. For $SrTiO_3$, the unrelaxed surface energies of the complementary SrO- and TiO_2-terminated (001) surfaces are thus equal by definition, as are those of the TiO- and Ba-terminated (011) surfaces. The relaxed surface energy is defined to be the energy of the unrelaxed surface plus the (negative) surface relaxation energy. These definitions are chosen for consistency with Refs. 8 and 31. Unlike the authors of Refs. 30, 32, and 56, we have made no effort to introduce chemical potentials here, so the results must be used with caution when addressing questions of the relative stability of surfaces with different stoichiometries.

In order to calculate the $SrTiO_3$ (001) surface energy, we started with the cleavage energy for unrelaxed SrO and TiO_2-terminated (001) surfaces. Surfaces with both terminations simultaneously arise under (001) cleavage of the crystal, and we adopt the convention that the cleavage energy is equally distributed between the created surfaces. In our cal-

TABLE VI. Surface rumpling s and relative displacements Δd_{ij} (in percent of the bulk lattice constant) for three near-surface planes of the TiO and O-terminated $SrTiO_3$ (011) surfaces.

	TiO terminated			O terminated	
	s	Δd_{12}	Δd_{23}	Δd_{12}	Δd_{23}
This study	11.28	−7.18	−0.67	−5.59	−0.23
Shell model[a]	14.47	−4.27	−3.86	−11.83	8.69

[a]Reference 19.

TABLE VII. Calculated cleavage, relaxation, and surface energies for $SrTiO_3$ (001) and (011) surfaces (in eV per surface cell). SM indicates the comparative results from the shell-model calculation of Ref. 19. In both cases, three near-surface planes were relaxed.

Surface	Termination	E_{cleav}	E_{rel}	E_{surf}	E_{surf}(SM)
$SrTiO_3$ (001)	TiO_2	1.39	−0.16	1.23	1.36
	SrO	1.39	−0.24	1.15	1.32
$SrTiO_3$ (011)	TiO	4.61	−1.55	3.06	2.21
	Sr	4.61	−1.95	2.66	3.04
	O	3.36	−1.32	2.04	1.54

culations, the seven-layer SrO-terminated (001) slab with 17 atoms and the TiO_2-terminated one with 18 atoms represent, together, seven bulk unit cells (35 atoms) so that

$$E_{surf}^{(unr)}(\Lambda) = \frac{1}{4}[E_{slab}^{(unr)}(SrO) + E_{slab}^{(unr)}(TiO_2) - 7E_{bulk}], \quad (1)$$

where Λ denotes SrO or TiO_2, $E_{slab}^{(unr)}(\Lambda)$ are the unrelaxed energies of the SrO- or TiO_2-terminated (001) slabs, E_{bulk} is the energy per bulk unit cell, and the factor of 4 comes from the fact that we create four surfaces upon the cleavage procedure. According to the results of our hybrid B3PW calculations, the cleavage results in a surface energy of 1.39 eV. Next, we can calculate the relaxation energies for each of the SrO and TiO_2 terminations, when both sides of the slabs relax, according to

$$E_{rel}(\Lambda) = \frac{1}{2}[E_{slab}^{(rel)}(\Lambda) - E_{slab}^{(unr)}(\Lambda)], \quad (2)$$

where $E_{slab}^{(rel)}(\Lambda)$ is the slab energy after relaxation (and again Λ=SrO or TiO_2). According to the results of our calculations, the SrO- and TiO_2-terminated surfaces relax by 0.24 and 0.16 eV respectively. The surface energy is then defined as the sum of the cleavage and relaxation energies,

$$E_{surf}(\Lambda) = E_{surf}^{(unr)}(\Lambda) + E_{rel}(\Lambda). \quad (3)$$

Our calculated surface energy for the SrO termination then comes to 1.15 eV, which is slightly smaller than the computed surface energy of 1.23 eV for the TiO_2 termination. The results are summarized in Table VII, wherein it can also be seen that we obtain slightly smaller surface energies than those obtained from the classical shell model[19] (1.32 and 1.36 eV for the SrO and TiO_2 terminations, respectively).

In order to calculate the $SrTiO_3$ (011) surface energies for the TiO- and Sr-terminated surfaces, we consider the cleavage of six bulk unit cells (30 atoms) to result in the TiO- and Sr-terminated slabs, containing 16 and 14 atoms, respectively, as shown in Figs. 3(d) and 3(e). We again divide the cleavage energy equally between these two surfaces and obtain

$$E_{surf}^{(unr)}(\Lambda) = \frac{1}{4}[E_{slab}^{(unr)}(Sr) + E_{slab}^{(unr)}(TiO) - 6E_{bulk}], \quad (4)$$

where Λ denotes Sr or TiO, $E_{slab}^{(unr)}(\Lambda)$ is the energy of the unrelaxed Sr or TiO terminated (011) slab, and E_{bulk} is the $SrTiO_3$ energy per bulk unit cell. Our calculated cleavage energy for the Sr- or TiO-terminated (011) surface is 4.61 eV. Next, we calculated the relaxation energies $E_{rel}(\Lambda)$ by using Eq. (2) for each of the Sr- and TiO-terminated surfaces, when both sides of slabs are allowed to relax. According to the results of our calculations, the relaxation energy of the Sr-terminated (011) surface is 1.95 eV, while that of the TiO-terminated surface is 1.55 eV. Thus, the surface relaxation energies are roughly ten times larger for the (011) surfaces than for the (001) surfaces. The surface energies are then obtained from Eq. (3), and the results are again summarized in Table VII.

Finally, when we cleave the $SrTiO_3$ crystal in another way, we obtain identical O-terminated (011) surface slabs containing 15 atoms each. This allows us to simplify the calculations since the unit cell of the seven-plane O-terminated (011) slab contains three bulk unit cells. Therefore, the relevant surface energy is

$$E_{surf}(O) = \frac{1}{2}[E_{slab}^{(rel)}(O) - 3E_{bulk}], \quad (5)$$

where $E_{surf}(O)$ and $E_{slab}^{(rel)}(O)$ are the surface energy and the relaxed slab total energy for the O-terminated (011) surface. Table VII gives our calculated surface energies.

Unlike for the (001) surface, we can see that different terminations of the (011) surface lead to large differences in the surface energies. Here, the lowest energy, according to our hybrid B3PW calculations, is 2.04 eV for the O-terminated surface. Our calculated surface energy of 3.06 eV for the TiO-terminated (011) surface is larger than that of the Sr-terminated (011) surface (2.66 eV). Note that, according to the classical shell-model calculations,[19] the O-terminated surface has the lowest energy (1.54 eV) of all of the three $SrTiO_3$ (011) surfaces. As we can see from Table VII, the O-terminated (011) surface energy is comparable to the (001) surface energies, both from our hybrid B3PW and from classical shell model[19] calculations.

E. $SrTiO_3$ (011) surface electronic structure

The interatomic bond populations for the three possible $SrTiO_3$ (011) surface terminations are given in Table VIII. The most important effect observed here is a strong increase in the Ti-O chemical bonding near the surface as compared to already large Ti-O bonding in the $SrTiO_3$ bulk. The most significant increase in the Ti-O chemical bonding occurs near the TiO-terminated (011) surface (0.130e), which is much

TABLE VIII. The A-B bond populations P (in e) and the relevant interatomic distances R (in Å) for three different $SrTiO_3$ (011) terminations. The symbols I–IV denote the number of each plane enumerated from the surface. The nearest-neighbor Ti-O distance in unrelaxed bulk $SrTiO_3$ is 1.952 Å.

Atom A	Atom B	P	R
	TiO-terminated (011) surface		
Ti(I)	O(I)	0.130	2.001
	O(II)	0.188	1.765
O(II)	Ti(III)	0.110	1.933
	Sr(III)	0.000	2.792
	O(III)	−0.024	2.801
Ti(III)	Sr(III)	0.000	3.382
	O(III)	0.106	1.955
	O(IV)	0.080	1.956
Sr(III)	O(III)	−0.010	2.760
	O(IV)	−0.014	2.720
O(III)	O(IV)	−0.028	2.712
	Sr-terminated (011) surface		
Sr(I)	O(II)	−0.044	2.534
O(II)	Sr(III)	−0.012	2.775
	Ti(III)	0.064	1.981
	O(III)	−0.042	2.802
Sr(III)	O(III)	−0.012	2.761
	O(IV)	−0.010	2.765
Ti(III)	O(III)	0.064	1.952
	Sr(III)	0.000	3.381
	O(IV)	0.092	1.951
O(III)	O(IV)	−0.048	2.739
	O-terminated (011) surface		
O(I)	Sr(II)	−0.012	2.641
	Ti(II)	0.146	1.682
	O(II)	−0.026	2.755
Sr(II)	O(II)	−0.042	2.546
	Ti(II)	0.000	3.217
Ti(II)	O(II)	0.080	2.000
	O(III)	0.100	1.776
O(II)	O(III)	0.002	2.898
Sr(II)	O(III)	−0.008	2.778
O(III)	O(IV)	−0.036	2.787
	Ti(IV)	0.060	1.989
	Sr(IV)	−0.016	2.705

stronger than the relevant Ti-O chemical bonding value near the TiO_2-terminated (001) surface (0.118e) and in the bulk (0.088e). For the O-terminated (011) surface, the O(I)-Ti(II) bond population is even larger (0.146e). The largest chemical bond population we found is between the Ti(I) and O(II) atoms in the surface-normal direction on the TiO-terminated (011) surface; it is roughly 50% larger than the Ti-O bond population near the TiO_2-terminated (001) surface, and slightly more than twice as large as the Ti-O bond population in the bulk. From Table VIII, we can see that for the TiO-terminated (011) surface, the Ti(I)-O(II) bond populations in the direction perpendicular to the surface (0.188e) are larger than those of the T(I)-O(I) chemical bond populations (0.130e) in the in-plane direction.

TABLE IX. Calculated Mulliken atomic charges Q (in e) and changes in atomic charges ΔQ with respect to the bulk charges (in e) for the three $SrTiO_3$ (011) surface terminations. The Mulliken atomic charges in the $SrTiO_3$ bulk are 2.351e for Ti, −1.407e for O, and 1.871e for Sr.

Atom (layer)	Q	ΔQ
	TiO-terminated (011) surface	
Ti(I)	2.211	−0.140
O(I)	−1.305	0.102
O(II)	−1.160	0.247
Sr(III)	1.843	−0.028
Ti(III)	2.333	−0.018
O(III)	−1.333	0.074
O(IV)	−1.429	−0.022
	Sr-terminated (011) surface	
Sr(I)	1.766	−0.105
O(II)	−1.560	−0.153
Sr(III)	1.874	0.003
Ti(III)	2.362	0.011
O(III)	−1.486	−0.079
O(IV)	−1.396	0.011
	O-terminated (011) surface	
O(I)	−1.172	0.235
Sr(II)	1.851	−0.020
Ti(II)	2.240	−0.111
O(II)	−1.461	−0.054
O(III)	−1.394	0.013
Sr(IV)	1.867	−0.004
Ti(IV)	2.332	−0.019
O(IV)	−1.433	−0.026

Table IX shows our calculated Mulliken effective charges Q and their changes ΔQ with respect to bulk $SrTiO_3$ for the three (011) terminations. The charge of the surface Ti atoms in the TiO-terminated (011) surface is reduced by 0.14e. Metal atoms in the third layer lose much less charge, with Sr and Ti atoms losing 0.028e and 0.018e, respectively. The O ions in the first, second, and third layers, except the central one, also have charges that are reduced by 0.102e, 0.247e, and 0.074e, respectively (i.e., they become less negative). In contrast, the central-layer O ions slightly increase their charges by 0.022e. The largest change is observed for subsurface O atoms (0.247e), which add up to contribute a large positive change of 0.494e in the subsurface layer.

In the case of the Sr-terminated (011) surface, negative changes in the charge are observed for all of the atoms except for oxygen in the central layer and metal atoms in the third layer. The largest changes occur for the subsurface O ion (−0.153e) and for the surface Sr ion (−0.105e). For the O-terminated (011) surface, the negative charge on the sur-

face oxygen is decreased ($\Delta Q=0.235e$). The net charge change in the second layer is negative ($-0.185e$) and mostly comes from the Ti ion ($-0.111e$). The O ion charge of the third layer is almost unchanged ($\Delta Q=0.013e$). The net charge change of the central-layer atoms is again negative but about four times smaller ($-0.049e$) than for the second layer, and now comes mostly from the charge change on the O ion ($-0.026e$).

IV. CONCLUSIONS

According to the results of our *ab initio* hybrid B3PW calculations, all of the upper layer atoms for the TiO_2- and SrO-terminated $SrTiO_3$ (001) surfaces, with the exception of the O atoms on the SrO-terminated surface, relax inward, whereas all of the second-layer atoms for both terminations relax outward. The outward relaxation of the second-layer O atoms on the TiO_2-terminated (001) surface, which is obtained in our current study, is in agreement with previous LDA calculations by Cheng *et al.*[16] but contradict LDA calculations of Padilla *et al.*[17] and SM calculations performed by Heifets *et al.*[19] Our large outward relaxation of the upper-layer O atoms is in good agreement with previous *ab initio* and SM[16,17,19] calculations for SrTiO3 (001) surfaces but is not typical for other ABO_3 perovskites since the upper-layer O atoms relax inward according to most *ab initio* studies.[18,33,57,58]

The inward displacement of the Sr on the SrO-terminated surface is about twice as large as that of the Ti atom on the TiO_2-terminated surface. Our computed surface rumpling for the SrO-terminated (001) surface is much larger than of the TiO_2-terminated (001) surface and is in excellent agreement with LEED[21] and RHEED[22] experimental results. Our calculations predict a compression of the distance between the first and second planes and an expansion for the second and third planes, which is in agreement with the results of previous *ab initio* and shell-model calculations. Our calculations, as well as all previous *ab initio* and shell-model calculations, agree with the LEED experiments regarding the compression of the distance between the first and second planes for the SrO-terminated surface but disagree with RHEED experiments. For the TiO_2-terminated surface, just the opposite is the case: our calculations and all of the previous *ab initio* and shell-model calculations agree with the RHEED[22] experiments regarding the sign of the interlayer relaxation between the second and third planes but disagree with LEED results.[21] The reason for this discrepancy is not clear, but it is discussed in Refs. 17 and 26. Thus, we conclude that in some cases, the disagreement between theoretical and experimental results should not be too seriously taken until the conflict between different experimental results is resolved.

For the $SrTiO_3$ (011) surface, we found that the relaxation magnitudes for the upper-layer metal atoms are considerably larger on the Sr and TiO-terminated surfaces than they are on the (001) surface upper-layer atoms. Whereas the metal atoms on the Sr- and TiO-terminated (011) surface strongly relax inward, the upper-layer oxygen atoms on the TiO-terminated (011) surface relax outward by 3.59% of the lattice constant a. The atomic displacements in the third plane from the surface for the three (011) terminations are still large. This is in sharp contrast to our results for the (001) surfaces, where the atomic displacements very quickly converge and are already small in the third layer. Our calculated surface rumpling for the TiO-terminated (011) surface is considerably larger than that of the SrO- or TiO_2-terminated (001) surfaces.

A comparison of our B3PW calculations to previous HF calculations by Heifets *et al.*[31] shows that the atomic displacement directions for TiO- and Sr-terminated (011) surfaces always coincide. The magnitudes of the atomic displacements are generally smaller in our B3PW calculations, with the exception of the upper-layer Ti atoms on the TiO-terminated (011) surface, and the third-layer O atoms on the Sr-terminated (011) surface, where the calculated atomic displacements are larger than in the HF calculations. There are also some qualitative difference in the case of the O-terminated (011) surface since the signs of the displacements differ in some cases between our hybrid B3PW calculations and the HF calculation, specifically for the y and z displacements of second-layer Sr atoms, and the y displacements of third-layer O atoms. Both calculations agree that the O-terminated surface has the lowest energy among the (011) surfaces studied, but while we find the TiO-terminated surface to have the highest energy, the HF calculations predict the Sr-terminated surface to have the highest energy.[31]

The SrO- and TiO_2-terminated $SrTiO_3$ (001) surfaces have comparable but small relaxation energies so that the surface energies assigned to them are similar (1.15 and 1.23 eV, respectively). On the other hand, the different terminations of the (011) surface have large cleavage and relaxation energies and large differences in the surface energies. The O-terminated surface has the lowest surface energy of the three (011) surfaces, although at 2.04 eV it is still significantly higher than that of the (001) terminations. The calculated surface energies of Sr-terminated (2.66 eV) and TiO-terminated (3.06 eV) (011) surfaces are both more than twice as large as those of the (001) surfaces.

Our *ab initio* calculations indicate a considerable increase in the Ti-O bond covalency near the (011) surface relative to the bulk, which is much larger than that of the (001) surface. The Ti-O bond populations are larger in the direction perpendicular to the TiO-terminated (011) surface than in the plane. Enhancement of covalency near surfaces is a common effect in ABO_3 perovskites; the enhancement of TiO covalency at $BaTiO_3$ and $PbTiO_3$ (001) and especially (011) surfaces was observed earlier in Ref. 33, and the enhancement of the Zr-O bond covalency at $BaZrO_3$ (001) and (011) surfaces was observed in Ref. 58. The increase in the Ti-O bond covalency at the surface, which is in agreement with the resonant photoemission experiments,[29] should have an impact on the electronic structure of surface defects (e.g., F centers), as well as affect the adsorption and surface diffusion of atoms and small molecules relevant to catalysis.

ACKNOWLEDGMENTS

The present work was supported by Deutsche Forschungsgemeinschaft (DFG) and by ONR Grant No. N00014-0-0054.

[1] J. F. Scott, *Ferroelectric Memories* (Springer, Berlin, 2000).
[2] A. E. Ring, S. E. Kesson, K. D. Reeve, D. M. Levins, and E. J. Ramm, in *Radioactive Waste Forms for the Further*, edited by W. Lutze and R. C. Ewings (North-Holland, Amsterdam, 1987).
[3] S. Kimura, J. Yamauchi, M. Tsukada, and S. Watanabe, Phys. Rev. B **51**, 11049 (1995).
[4] Z. Q. Li, J. L. Zhu, C. Q. Wu, Z. Tang, and Y. Kawazoe, Phys. Rev. B **58**, 8075 (1998).
[5] R. Herger, P. R. Willmott, O. Bunk, C. M. Schlepütz, B. D. Patterson, and B. Delley, Phys. Rev. Lett. **98**, 076102 (2007).
[6] N. Erdman, K. Poeppelmeier, M. Asta, O. Warschkow, D. E. Ellis, and L. Marks, Nature (London) **419**, 55 (2002).
[7] T. Kubo and H. Nozoye, Surf. Sci. **542**, 177 (2003).
[8] E. Heifets, R. I. Eglitis, E. A. Kotomin, J. Maier, and G. Borstel, Phys. Rev. B **64**, 235417 (2001).
[9] E. Heifets, R. I. Eglitis, E. A. Kotomin, J. Maier, and G. Borstel, Surf. Sci. **513**, 211 (2002).
[10] K. Johnston, M. R. Castell, A. T. Paxton, and M. W. Finnis, Phys. Rev. B **70**, 085415 (2004).
[11] R. I. Eglitis, S. Piskunov, E. Heifets, E. A. Kotomin, and G. Borstel, Ceram. Int. **30**, 1989 (2004).
[12] S. Piskunov, E. A. Kotomin, E. Heifets, J. Maier, R. I. Eglitis, and G. Borstel, Surf. Sci. **575**, 75 (2005).
[13] R. Herger, P. R. Willmott, O. Bunk, C. M. Schlepütz, B. D. Patterson, B. Delley, V. L. Shneerson, P. F. Lyman, and D. K. Saldin, Phys. Rev. B **76**, 195435 (2007).
[14] C. H. Lanier, A. van de Walle, N. Erdman, E. Landree, O. Warschkow, A. Kazimirov, K. R. Poeppelmeier, J. Zegenhagen, M. Asta, and L. D. Marks, Phys. Rev. B **76**, 045421 (2007).
[15] Y. L. Li, S. Choudhury, J. H. Haeni, M. D. Biegalski, A. Vasudevarao, A. Sharan, H. Z. Ma, J. Levy, V. Gopalan, S. Trolier-McKinstry, D. G. Schlom, Q. X. Jia, and L. Q. Chen, Phys. Rev. B **73**, 184112 (2006).
[16] C. Cheng, K. Kunc, and M. H. Lee, Phys. Rev. B **62**, 10409 (2000).
[17] J. Padilla and D. Vanderbilt, Surf. Sci. **418**, 64 (1998).
[18] B. Meyer, J. Padilla, and D. Vanderbilt, Faraday Discuss. **114**, 395 (1999).
[19] E. Heifets, E. A. Kotomin, and J. Maier, Surf. Sci. **462**, 19 (2000).
[20] V. Ravikumar, D. Wolf, and V. P. Dravid, Phys. Rev. Lett. **74**, 960 (1995).
[21] N. Bickel, G. Schmidt, K. Heinz, and K. Müller, Phys. Rev. Lett. **62**, 2009 (1989).
[22] T. Hikita, T. Hanada, M. Kudo, and M. Kawai, Surf. Sci. **287–288**, 377 (1993).
[23] M. Kudo, T. Hikita, T. Hanada, R. Sekine, and M. Kawai, Surf. Interface Anal. **22**, 412 (1994).
[24] Y. Kido, T. Nishimura, Y. Hoshido, and H. Mamba, Nucl. Instrum. Methods Phys. Res. B **161-163**, 371 (2000).
[25] A. Ikeda, T. Nishimura, T. Morishita, and Y. Kido, Surf. Sci. **433**, 520 (1999).
[26] G. Charlton, S. Brennan, C. A. Muryn, R. McGrath, D. Norman, T. S. Turner, and G. Thorthon, Surf. Sci. **457**, L376 (2000).
[27] P. A. W. van der Heide, Q. D. Jiang, Y. S. Kim, and J. W. Rabalais, Surf. Sci. **473**, 59 (2001).
[28] W. Maus-Friedrichs, M. Frerichs, A. Gunhold, S. Krischok, V. Kempter, and G. Bihlmayer, Surf. Sci. **515**, 499 (2002).
[29] R. Courths, B. Cord, and H. Saalfeld, Solid State Commun. **70**, 1047 (1989).
[30] F. Bottin, F. Finocchi, and C. Noguera, Phys. Rev. B **68**, 035418 (2003).
[31] E. Heifets, W. A. Goddard III, E. A. Kotomin, R. I. Eglitis, and G. Borstel, Phys. Rev. B **69**, 035408 (2004).
[32] E. Heifets, J. Ho, and B. Merinov, Phys. Rev. B **75**, 155431 (2007).
[33] R. I. Eglitis and D. Vanderbilt, Phys. Rev. B **76**, 155439 (2007).
[34] S. Piskunov, E. Heifets, R. I. Eglitis, and G. Borstel, Comput. Mater. Sci. **29**, 165 (2004).
[35] H. Shi, R. I. Eglitis, and G. Borstel, Phys. Rev. B **72**, 045109 (2005).
[36] H. Shi, R. I. Eglitis, and G. Borstel, J. Phys.: Condens. Matter **18**, 8367 (2006).
[37] However, in the LDA calculation of Bottin *et al.* (Ref. 30), the lattice constant of 3.951 Å is similar to the Hartree–Fock one.
[38] R. D. King-Smith and D. Vanderbilt, Phys. Rev. B **49**, 5828 (1994).
[39] W. Zhong and D. Vanderbilt, Phys. Rev. Lett. **74**, 2587 (1995); Phys. Rev. B **53**, 5047 (1996).
[40] C. LaSota, C. Z. Wang, R. Yu, and H. Krakauer, Ferroelectrics **194**, 109 (1997).
[41] N. Sai and D. Vanderbilt, Phys. Rev. B **62**, 13942 (2000).
[42] V. R. Saunders, R. Dovesi, C. Roetti, M. Causa, N. M. Harrison, R. Orlando, and C. M. Zicovich-Wilson, *CRYSTAL-2003 User Manual* (University of Torino, Torino, Italy, 2003).
[43] A. D. Becke, J. Chem. Phys. **98**, 5648 (1993).
[44] J. P. Perdew and Y. Wang, Phys. Rev. B **33**, 8800 (1986); **40**, 3399(E) (1989); **45**, 13244 (1992).
[45] P. J. Hay and W. R. Wadt, J. Chem. Phys. **82**, 270 (1985); P. J. Hay and W. R. Wadt, *ibid.* **82**, 284 (1984); P. J. Hay and W. R. Wadt, *ibid.* **82**, 299 (1984).
[46] H. J. Monkhorst and J. D. Pack, Phys. Rev. B **13**, 5188 (1976).
[47] C. Noguera, J. Phys.: Condens. Matter **12**, R367 (2000).
[48] P. W. Tasker, J. Phys. C **12**, 4977 (1979).
[49] A. Pojani, F. Finocchi, and C. Noguera, Surf. Sci. **442**, 179 (1999).
[50] B. J. Kennedy, C. J. Howard, and B. Chakoumakos, J. Phys.: Condens. Matter **11**, 1479 (1999).
[51] J. C. Boettger, Phys. Rev. B **49**, 16798 (1994).
[52] V. Fiorentini and M. Methfessel, J. Phys.: Condens. Matter **8**, 6525 (1996).
[53] *Ferroelectrics and Related Substances*, Landolt-Bornstein, New Series, Group III, Vol. 3, edited by K. H. Hellwege and A. M. Hellwege (Springer-Verlag, Berlin, 1969).
[54] C. R. A. Catlow and A. M. Stoneham, J. Phys. C **16**, 4321 (1983).
[55] R. C. Bochicchio, and H. F. Reale, J. Phys. B **26**, 4871 (1993).
[56] K. Rapcewicz, B. Chen, B. Yakobson, and J. Bernholc, Phys. Rev. B **57**, 7281 (1998).
[57] J. Padilla and D. Vanderbilt, Phys. Rev. B **56**, 1625 (1997).
[58] R. I. Eglitis, J. Phys.: Condens. Matter **19**, 356004 (2007).